African Health Sciences Bulletin

Article

Drug Repositioning in Epidermal Growth Factor Receptor Inhibitors

Yoongho Lim[1,2]

[1]Research Center, Eswatini Medical Christian University, Mbabane, Kingdom of Eswatini
[2]Division of Bioscience and Biotechnology, Konkuk University, Seoul 05029, Republic of Korea

*Correspondence to Y Lim; yoongho@konkuk.ac.kr

Abstract: Epidermal growth factor receptor has been used as a targeted therapy for non-small-cell lung cancer. Many inhibitors of epidermal growth factor receptor have been developed for the treatment of non-small-cell lung cancer and are in clinical use. Due to their resistance against epidermal growth factor receptor, however, the development of new inhibitors is required. To overcome problems including costly, laborious, and time-consuming processes for new drug development, recently, drug repositioning is emerging as a new alternative in the drug discovery. In this study, therefore, drug repositioning based on virtual screening and *in silico* docking methods was applied for finding new inhibitors of epidermal growth factor receptor.

Keywords: epidermal growth factor receptor; drug repositioning; virtual screening; *in silico* docking

1. Introduction

Lung cancer, a common tumor, accounts for 30% of all cancer-related deaths [1]. Majority of lung cancers are known to belong to non-small-cell lung cancer (NSCLC). Epidermal growth factor receptor (EGFR) has been found to be overexpressed in a variety of tumor cells [2]. Overexpression of EGFR in NSCLC has been found to reduce survival [3]. EGFR belongs to the ErbB family including EGFR/ErbB-1, HER2/ErbB-2, HER3/ErbB-3, and HER4/ErbB-4 [4]. Transforming growth factor-alpha (TGF-α) and epidermal growth factor (EGF) bind to the extracellular domain of EGFR as a ligand. They induce a conformational change and dimerization of the receptor, and activate the intracellular tyrosine kinase [5]. Then the receptor, EGFR transduces cellular responses through its signaling pathways [6]. Activation of the EGFR pathway results in tumor growth and progression [7]. Therefore, EGFR has been used as a targeted therapy for NSCLC.

EGFR consists of a transmembrane domain, an extracellular EGF binding domain, and a cytoplasmic domain which is composed of a C-terminal phosphorylation subunit and a protein tyrosine kinase subunit [8]. Because inhibiting EGFR can reduce tumor growth and progression, approaches to inhibit EGFR signaling have been studies. Two possible methods are for small molecules to inhibit the activity of the intracellular tyrosine kinase and for a ligand to bind the extracellular domain with a monoclonal antibody (mAb) [4]. As tyrosine kinase inhibitors, gefitinib, erlotinib, lapatinib, and vandetanib have been known [2]. Due to their resistance against EGFR, however, the development of new inhibitors is required.

Food and Drug Administration (FDA) of the United States presents five stages of new drug development as follows: "(1) discovery and development, (2) preclinical research, (3) clinical research, (4) FDA review, and (5) FDA post-market safety monitoring" [9]. This is an extremely costly, laborious, and time-consuming process. About 90% of drug candidates fail during phase 1 clinical trials [10]. In order to overcome such problems, recently, drug repositioning is emerging as a new alternative in the drug discovery. Unlike the traditional drug development, drug repositioning includes identification of the compounds, attainment, development, and FDA post-market safety monitoring [11]. The aim of drug repositioning is to find new therapeutic indications for drugs that have already been approved for use. As a result, an extremely costly, laborious, and time-consuming process required for the traditional drug development can be reduced. As shown in Fig.1, the publications in drug repositioning reported in PubMed have been increasing rapidly since 2010. In this study, In this study, therefore, drug repositioning based on virtual screening and *in silico* docking methods was applied for finding new EGFR inhibitors.

Received 19 June 2023; Revised 29 June 2023; Accepted 1 July 2023

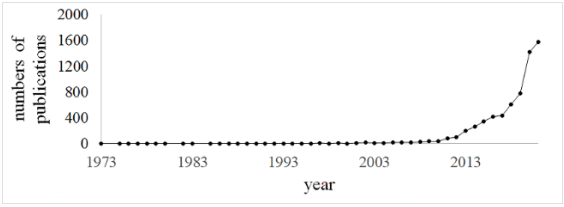

Fig. 1. Publications in the field of drug repositioning reported in PubMed.

2. Materials and Methods

2.1. virtual screening

Virtual screening was carried out using LEA3D web server (https://chemoinfo.ipmc.cnrs.fr/LEA3D) [12]. As ligands for virtual screening, 2056 drugs that have already been approved by the Food and Drug Administration (FDA) were used. They were ranked based on the scoring function provided by LEA3D web server. The target protein for virtual screening was wild type EGFR. Of many three-dimensional (3D) structures deposited in the protein data bank, 6vhn.pdb was selected because it consists of wild type EGFR kinase domain [13]. The coordinates of the center of the binding site for the docking process of virtual screening were determined with the help of AutoDock vina program (Scripps Research Institute, La Jolla, San Diego, USA) as follows : x = -53.389, y = -1.361, z = 23.694 [14]. Likewise, the size of the grid box for the binding site was determined using AutoDock vina as follows: x = 24Å, y = 20Å, z = 18Å.

2.2. in silico docking

Because the scores provided by the LEA3D web server are determined based on the docking results as well as other factors, *in silico* docking experiments for drugs with high scores were performed in this study. It was carried out using AutoDock vina and Chimera [15], and its detailed experimental method followed the method published previously [16]. The docking results were analyzed using the LigPlot program [17], and 3D images were generated by the PyMOL program (The PyMOL Molecular Graphics System, Version 1.2r3pre, Schrödinger, LLC.).

2.3. target prediction

In order to elucidate the off-target effects of the drugs for repositioning, SwissTargetPrediction web server (http://www.swisstargetprediction.ch/) was used [18].

3. Results and Discussion

3.1. fulvestrant

LEA3D web server ranked 2058 drugs approved by the FDA. The first drug ranked by the scoring function of LEA3D web server is fulvestrant, (7R,8R,9S,13S,14S,17S)-13-methyl-7-[9-(4,4,5,5,5-pentafluoropentylsulfinyl)nonyl]-6,7,8,9,11,12,14,15,16,17-decahydrocyclopenta[a]phenanthrene-3,17-diol. Its structure is shown in Fig. 2.

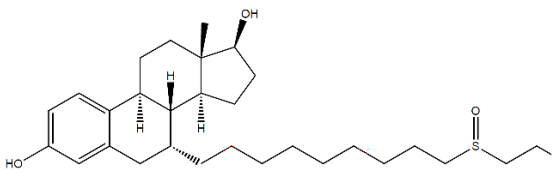

Fig. 2. The structure of fulvestrant, (7R,8R,9S,13S,14S,17S)-13-methyl-7-[9-(4,4,5,5,5-pentafluoropentylsulfinyl)nonyl]-6,7,8,9,11,12,14,15,16,17-decahydrocyclopenta[a]phenanthrene-3,17-diol.

To evaluate whether fulvestrant is docked into EGFR well, *in silico* docking experiments were carried out. The 3D structure of EGFR was selected from the protein data bank (PDB). It was 6vhn.pdb where N-[3-({4-[4-(4-fluorophenyl)-2-(methylsulfanyl)-1H-imidazol-5-yl]pyridin-2-yl}amino)-4-methoxyphenyl]propenamide (named as QQJ) is contained as its ligand [Fig. 3] [13].

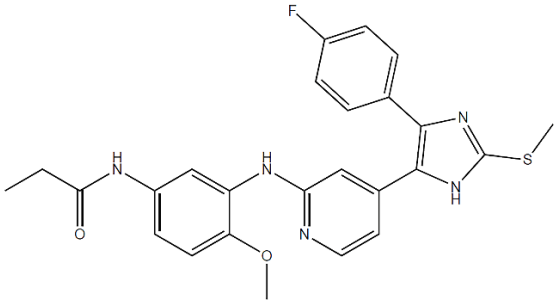

Fig. 3. The structure of N-[3-({4-[4-(4-fluorophenyl)-2-(methylsulfanyl)-1H-imidazol-5-yl]pyridin-2-yl}amino)-4-methoxyphenyl]propenamide (named as QQJ) contained in 6vhn.pdb (EGFR) as a ligand.

For *in silico* docking, the AutoDock vina program was used. First, the holo-protein of EGFR was prepared using the Chimera program by deleting the ligand from the X-ray crystallographic structure deposited in the PDB (6vhn.pdb). The binding site for *in silico* docking was determined using AutoDock vina. To confirm whether the current docking procedure is reliable, the ligand contained in 6vhn.pdb was docked in the holo-protein. The binding energy of the ligand QQJ ranged between -9.0 and -8.2 kcal/mol. The root mean square deviation (RMSD) between the QQJ – holo-protein complex obtained from *in silico* docking and 6vhn.pdb was determined using the Chimera program and it was 1.8Å. Even though the docking pose of the ligand contained in the complex obtained from *in silico* docking showed a little difference in propenamide group as shown in Fig. 4, the binding energy of the ligand QQJ was low and the ligand was docked in the binding pocket well, so it can be considered that this docking procedure is reliable.

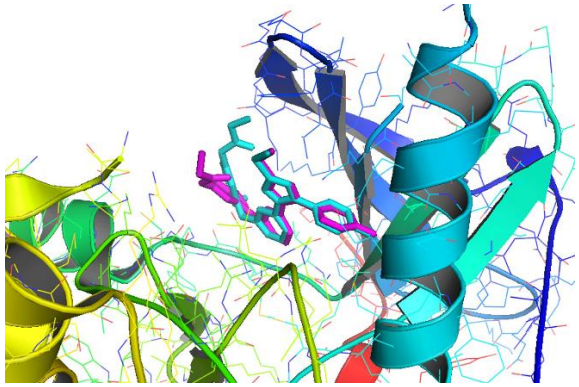

Fig. 4. Superimposition of the ligand (magenta) contained in 6vhn.pdb with that (cyan) in the QQJ – holo-protein complex obtained from the *in silico* docking procedure. The 3D image was generated by the PyMOL program.

In order to dock fulvestrant into the holo-protein of EGFR, first, its 3D structure was obtained from PubChem (CID = 104741, https://pubchem.ncbi.nlm.nih.gov/). The binding energy of fulvestrant to holo-protein of EGFR ranged between -7.0 and -6.0 kcal/mol. The RMSD between 6vhn.pdb and the EGFR holo-protein – fulvestrant complex was 3.4Å. This value was obtained based on a comparison of the ligand of 6vhn.pdb and with fulvestrant contained in the fulvestrant - EGFR complex. Even fulvestrant was docked into the binding pocket of EGFR well, its docking pose was different from that of the ligand QQJ contained in 6vhn.pdb [Fig. 5].

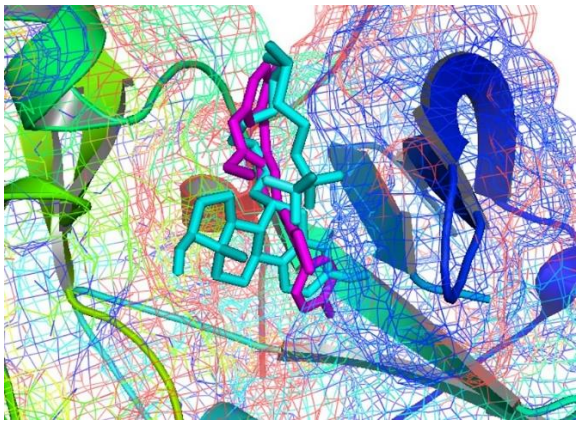

Fig. 5. The superimposed image of fulvestrant (cyan) and QQJ (magenta) in the binding site of EGFR.

To elucidate the binding condition, the hydrophobic interactions and hydrogen bonds between the ligand QQJ contained in 6vhn.pdb (EGFR) and the residues of the target protein EGFR were analyzed using the LigPlot program [Fig. 6].

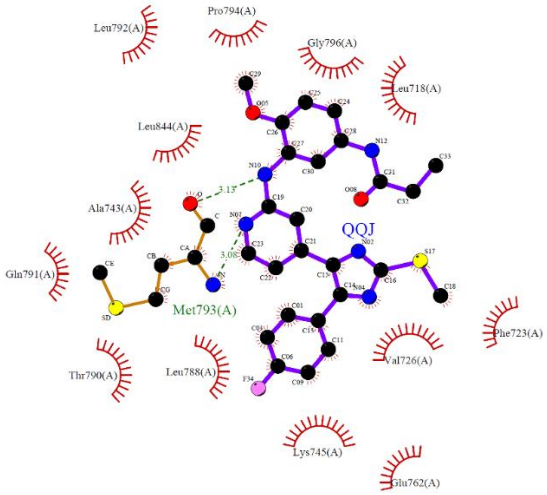

Fig. 6. Interactions between the ligand QQJ contained in 6vhn.pdb (EGFR) and residues of 6vhn.pdb analyzed using the LigPlot program. The crescent-shaped red mark denotes the residues participating in hydrophobic interactions, and the green dotted lines represent hydrogen bonds.

Thirteen residues including L718, F723, V726, A743, K745, E762, L788, T790, E791, L792, P794, G796, L844 of EGFR participated in hydrophobic interactions with the ligand QQJ contained in 6vhn.pdb (EGFR). The LigPlot analysis showed there are two hydrogen bonds (H-bonds) between oxygen of M793 and amino group connected between benzene ring of methoxyphenylpropanamide and pyridine (3.13Å), and between nitrogen of M793 and nitrogen of pyridine. However, because there is no hydrogen between nitrogen of M793 and nitrogen of pyridine, to confirm these results obtained by LigPlot, H-bonds were analyzed using the PyMOL program again. This resulted in only H-bond between oxygen of M793 and amino group connected between benzene ring of methoxyphenylpropanamide and pyridine [Fig. 7].

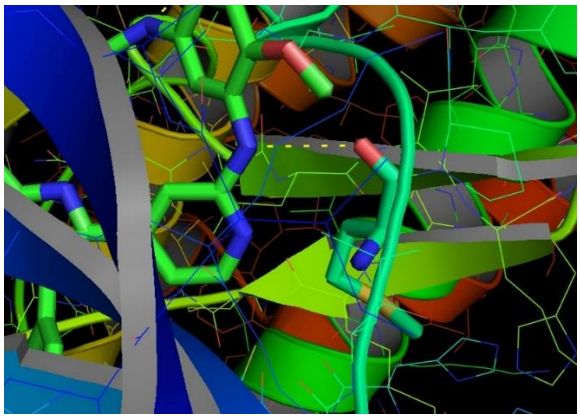

Fig. 7. The hydrogen bond generated by the PyMOL program. The left molecule represented by the stick is QQJ, and the right residue by the stick is M793. The yellow dotted line denotes the hydrogen bond.

Interactions between fulvestrant and EGFR were analyzed using LigPlot [Fig. 8]. Seven residues including L718, V726, T790, M793, G796, L844, T854 participated in hydrophobic interactions with fulvestrant. Five hydrogen bonds with fulvestrant exist : hydroxyl group of N842 and hydroxy group of cyclopentane (2.78Å), oxygen of peptide bond of R841 and hydroxy group of cyclopentane (3.02Å), nitrogen of peptide bond of K745 and hydroxy group of phenanthrene (3.19Å), oxygen of peptide bond of L788 and hydroxy group of phenanthrene (2.67Å), and oxygen of peptide bond of A743 and hydroxy group of phenanthrene (3.16Å).

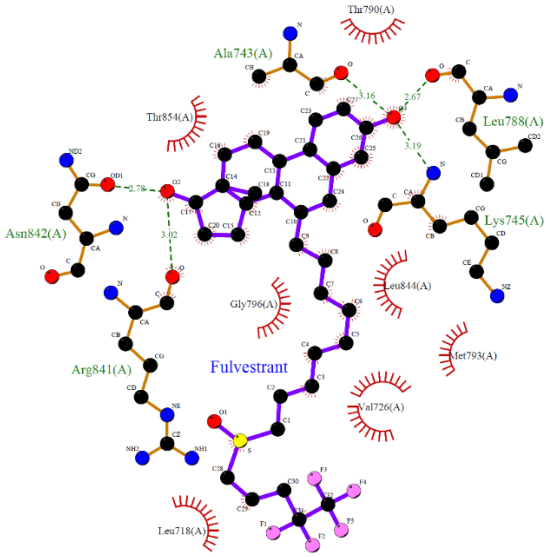

Fig. 8. Interactions between fulvestrant and residues of 6vhn.pdb (EGFR) analyzed using the LigPlot program.

While in the case of QQJ, 14 residues participated in the interactions with EGFR, in fulvestrant, 12 residues did. The binding energy between QQJ and EGFR (-9.0 kcal/mol) is better than that of fulvestrant (-7.0 kcal/mol). The number of residues participating in the interaction between the ligand and the target protein may explain the difference of the binding energies. To compare the docking pose of fulvestrant with that of QQJ contained in 6vhn.pdb as a ligand, fulvestrant in the binding site was superimposed with QQJ. As shown in Fig. 9, the docking pose of fulvestrant is similar to that of QQJ.

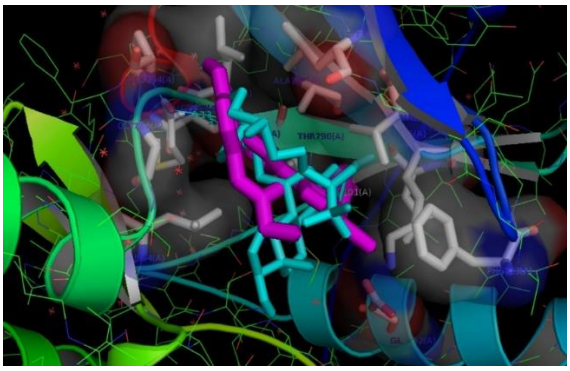

Fig. 9. The 3D images of fulvestrant (cyan) and QQJ (magenta) contained in the binding pocket of 6vhn.pdb (EGFR) generated using the PyMol program. The white colored residues represented by the stick denote the residues participated in the interactions between fulvestrant and EGFR analyzed by LigPlot.

In order to elucidate the off-target effects of fulvestrant, SwissTargetPrediction web server was used. Nine proteins were predicted to be the targets of fulvestrant, but the probability that they can be targets ranged between 0.44 and 0.07 [Table 1]. Therefore, it can be considered that there is no off-target effects of fulvestrant.

Table 1. The targets of fulvestrant predicted by SwissTargetPrediction web server.

Target	Target Class	Probability
Bile acid receptor FXR	Nuclear receptor	0.44
Estrogen receptor alpha	Nuclear receptor	0.44
Progesterone receptor	Nuclear receptor	0.44
Epoxide hydratase	Protease	0.44
Estrogen receptor beta	Nuclear receptor	0.44
Pregnane X receptor	Nuclear receptor	0.44
Estrogen-related receptor alpha	Nuclear receptor	0.44
Estradiol 17-beta-dehydrogenase 1	Enzyme	0.07
Androgen Receptor	Nuclear receptor	0.07

Even embryo-fetal toxicity of fulvestrant whose brand name is Faslodex was reported [19], it was approved by FDA in the United States for “treatment of hormone receptor (HR)-positive, human epidermal growth factor receptor 2 -negative advanced breast cancer in postmenopausal women not previously treated with endocrine therapy, or treatment of HR-positive advanced breast cancer in postmenopausal women with disease progression following endocrine therapy” (FDA Reference ID: 4144559, 2002). It was developed by AstraZeneca. It has been known as a selective estrogen receptor degrader, but not known to be an inhibitor of EGFR. In this study, it was docked into EGFR well and its off-target effects could be predicted to be very low. As a result, fulvestrant can be repositioned as an EGFR inhibitor.

3.2. elbasvir

The second drug ranked by the scoring function of LEA3D web server is elbasvir. Zepatier developed by Merck is a fixed-dose combination product containing elbasvir and grazoprevir [20]. The former is a hepatitis C virus (HCV) nonstructural protein 5A (NS5A) inhibitor, and the latter, an HCV NS3/4A protease inhibitor (FDA Reference ID: 4055857, 2016). The name of elbasvir is methyl N-[(2S)-1-[(2S)-2-[5-[(6S)-3-[2-[(2S)-1-[(2S)-2-(methoxycarbonylamino)-3-methylbutanoyl]pyrrolidin-2-yl]-1H-imidazol-5-yl]-6-phenyl-6H-indolo[1,2-c][1,3]benzoxazin-10-yl]-1H-imidazol-2-yl]pyrrolidin-1-yl]-3-methyl-1-oxobutan-2-yl]carbamate and its structure is shown in Fig. 10.

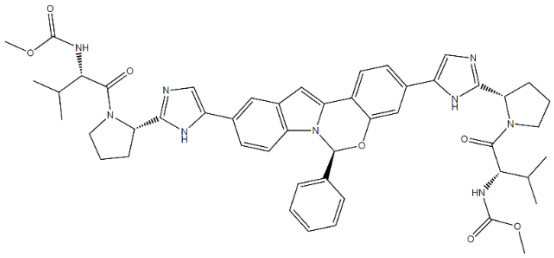

Fig. 10. The structure of elbasvir, methyl N-[(2S)-1-[(2S)-2-[5-[(6S)-3-[2-[(2S)-1-[(2S)-2-(methoxycarbonylamino)-3-methylbutanoyl]pyrrolidin-2-yl]-1H-imidazol-5-yl]-6-phenyl-6H-indolo[1,2-c][1,3]benzoxazin-10-yl]-1H-imidazol-2-yl]pyrrolidin-1-yl]-3-methyl-1-oxobutan-2-yl]carbamate.

In order to confirm whether elbasvir is docked into EGFR, *in silico* docking was carried out. Even though the docking process by AutoDock vina provides nine docking complexes, in the case of elbasvir, only one docking complex was generated. Its binding energy was -6.0 kcal/mol. As shown in Fig. 11, its docking pose was not good. Even it was docked in the binding pocket, it was placed in the entrance of the binding pocket and was not superimposed with QQJ contained in 6vhn.pdb (EGFR) as a ligand.

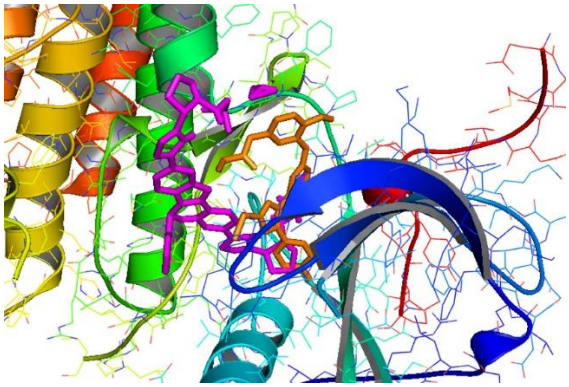

Fig. 11. The 3D images of elbasvir (magenta) and QQJ (orange) contained in the binding pocket of 6vhn.pdb (EGFR) generated using the PyMol program.

Elbasvir was predicted to bind multiple SARS-CoV-2 proteins using computational target-based drug repurposing methods [21]. However, based on the current docking study, elbasvir cannot be used as a repositioning drug for EGFR.

3.3. saquinavir

The scoring function of LEA3D web server provided saquinavir as the third drug repositioned for EGFR, which was developed by Roche. It is (2S)-N-[(2S,3R)-4-[(3S,4aS,8aS)-3-(tert-butylcarbamoyl)-3,4,4a,5,6,7,8,8a-octahydro-1H-isoquinolin-2-yl]-3-hydroxy-1-phenylbutan-2-yl]-2-(quinoline-2-carbonylamino)butanediamide and its structure is shown in Fig. 12.

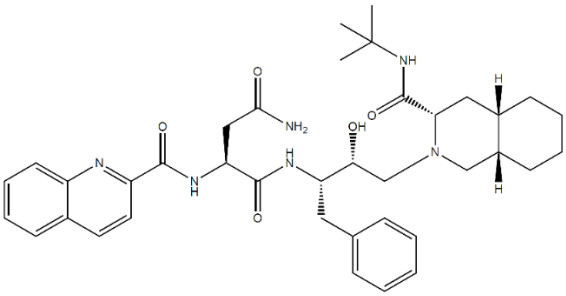

Fig. 12. The structure of saquinavir, (2S)-N-[(2S,3R)-4-[(3S,4aS,8aS)-3-(tert-butylcarbamoyl)-3,4,4a,5,6,7,8,8a-octahydro-1H-isoquinolin-2-yl]-3-hydroxy-1-phenylbutan-2-yl]-2-(quinoline-2-carbonylamino)butanediamide.

To confirm whether it is docked into EGFR, *in silico* docking was performed. Its binding energy ranged between -8.3 kcal/mol and -7.4 kcal/mol. The RMSD between 6vhn.pdb and the EGFR holo-protein – saquinavir complex was 1.9Å. It was docked into the binding pocket of EGFR well and was superimposed with the ligand of 6vhn.pdb, QQJ well [Fig. 13].

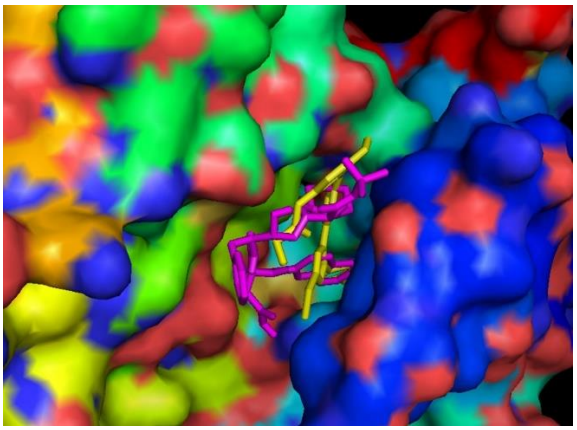

Fig. 13. The 3D images of saquinavir (magenta) and QQJ (orange) contained in the binding pocket of 6vhn.pdb (EGFR) generated using the PyMol program.

Because saquinavir was docked into EGFR well, the interaction between saquinavir and EGFR was analyzed using LigPlot. Fifteen residues including L718, F723, V726, A743, K745, E762, L788, T790, L792, M793, C797, R841, N842, L844, and D855 of EGFR participated in hydrophobic interactions with saquinavir [Fig. 14]. Two hydrogen bonds were observed as follows: hydroxy group of D800 and hydroxy group of saquinavir (3.27Å), and hydroxy group of T854 and ketone of quinoline-2-carbonylamino group of saquinavir (3.33Å). In the case of QQJ contained in 6vhn.pdb as a ligand, thirteen residues including L718, F723, V726, A743, K745, E762, L788, T790, E791, L792, P794, G796, L844 of EGFR participated in hydrophobic interactions, and one hydrogen bond between oxygen of M793 and amino group connected between benzene ring of methoxyphenylpropanamide and pyridine was observed. Instead of three residues including E791, P794, and G796 of QQJ, five residues including M793, C797, R841, N842, and D855 participated in hydrophobic interactions of saquinavir. While M793 forms the H-bond in QQJ, T854 and D800 do H-bonds in saquinavir. In order to look into the residues surrounding saquinavir in detail, the 3D image of the binding site showing saquinavir (magenta) and residues analyzed by LigPlot (white sticks) was generated using the PyMOL program where green dot lines denote hydrogen bonds [Fig. 15]. As a result, saquinavir is predicted to bind to EGFR better than QQJ contained in 6vhn.pdb.

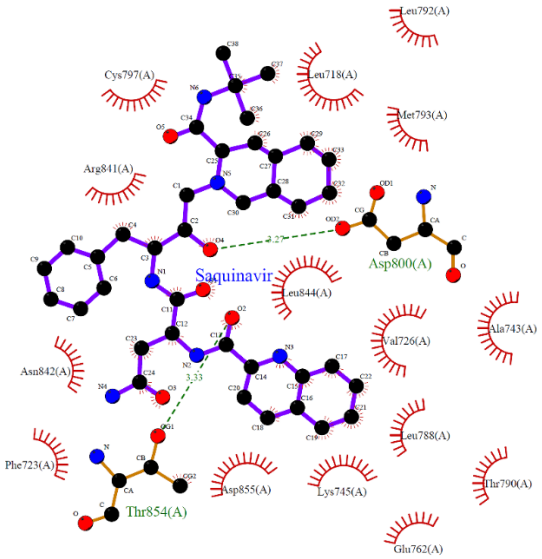

Fig. 14. Interactions between saquinavir and residues of 6vhn.pdb analyzed using the LigPlot program. The crescent-shaped red mark denotes the residues participating in hydrophobic interactions, and the green dotted lines represent hydrogen bonds.

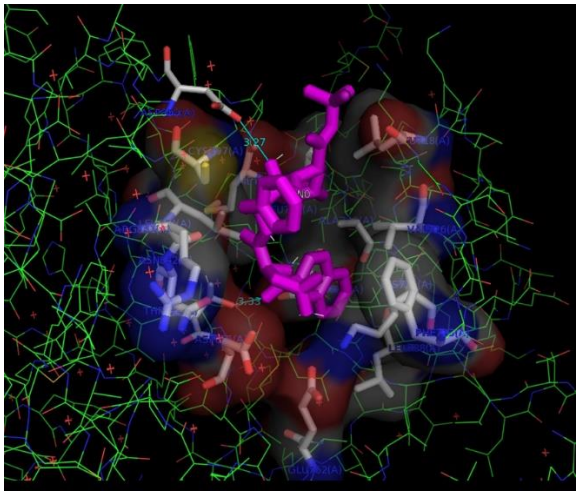

Fig. 15. The 3D image of the binding site showing saquinavir (magenta) and residues analyzed by LigPlot (white sticks) generated using the PyMOL program where green dot lines denote hydrogen bonds.

The off-target effects of saquinavir were elucidated with the help of SwissTargetPrediction web server. More than a hundred proteins were predicted to be the targets of saquinavir. Because the probability of seven target proteins including Thromboxane-A synthase, Vasopressin V1a receptor, Neurokinin 2 receptor, Mu opioid receptor, Dopamine D3 receptor, Delta opioid receptor, and Kappa Opioid receptor is one, even the probability of other proteins is less than 0.22, there may be predicted to be off-target effects in saquinavir [Table 2].

Table 2. The target proteins of saquinavir predicted by SwissTargetPrediction web server.

Target	Target Class	Probability
Thromboxane-A synthase	Cytochrome P450	1
Vasopressin V1a receptor	Family A G protein-coupled receptor	1
Neurokinin 2 receptor	Family A G protein-coupled receptor	1
Mu opioid receptor	Family A G protein-coupled receptor	1
Dopamine D3 receptor	Family A G protein-coupled receptor	1
Delta opioid receptor	Family A G protein-coupled receptor	1
Kappa Opioid receptor	Family A G protein-coupled receptor	1
Cathepsin D	Protease	0.22

Saquinavir is an human immunodeficiency virus (HIV) protease inhibitor used for the HIV-1 treatment in combination with other antiretroviral agents. Its mesylate compound was approved by FDA in 1995 (FDA Reference ID: 3223879, 1995) [22]. Its brand name is Invirase. Because of the competition from other anti-HIV medications, nowadays it was discontinued. As mentioned above, SwissTargetPrediction web server provided several proteins which can target saquinavir, but there was no EGFR. In the current study, saquinavir was docked into EGFR well, thus it can be repositioned for EGFR.

3.4. ritonavir

The fourth ranked drug generated based on the scoring function of LEA3D web server was ritonavir, a protease inhibitor, developed by AbbVie. It was approved for the treatment of pediatric patients with HIV-1 infection in combination with other antiretroviral agents by FDA in 1996 (FDA Reference ID: 4108604, 1996) [23]. Its name is 1,3-thiazol-5-ylmethyl N-[(2S,3S,5S)-3-hydroxy-5-[[(2S)-3-methyl-2-[[methyl-[(2-propan-2-yl-1,3-thiazol-4-yl)methyl]carbamoyl]amino]butanoyl]amino]-1,6-diphenylhexan-2-yl]carbamate, and its brand name is Norvir. Its structure is shown in Fig. 16.

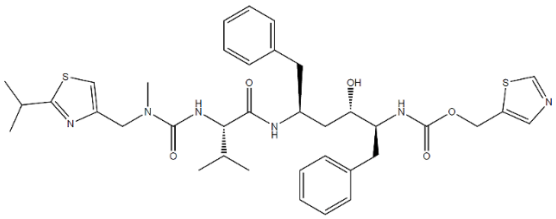

Fig. 16. The structure of ritonavir, 1,3-thiazol-5-ylmethyl N-[(2S,3S,5S)-3-hydroxy-5-[[(2S)-3-methyl-2-[[methyl-[(2-propan-2-yl-1,3-thiazol-4-yl)methyl]carbamoyl]amino]butanoyl]amino]-1,6-diphenylhexan-2-yl]carbamate.

The results obtained from *in silico* docking showed that the binding energy ranged between -7.7 kcal/mol and -7.0 kcal/mol. The RMSD between 6vhn.pdb and the EGFR holo-protein – ritonavir complex was 3.2Å. As shown in Fig. 17, ritonavir was docked into EGFR well.

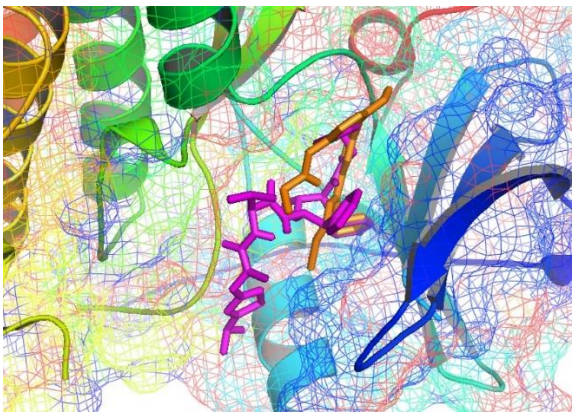

Fig. 17. Superimposition of ritonavir (magenta) and QQJ (orange) contained in the binding pocket of 6vhn.pdb (EGFR) generated using the PyMol program.

The analysis by LigPlot displayed there are sixteen hydrophobic interactions and one hydrogen bond between ritonavir and EGFR [Fig. 18]. L718, G719, F723, V726, A743, K745, E762, M766, L788, T790, M793, G796, R841, L844, D855, and G857 are included in the hydrophobic interactions, and hydroxy group of T854 and hydroxy group of ritonavir form a hydrogen bond (2.75Å). In the case of QQJ contained in 6vhn.pdb as a ligand, thirteen residues participated in hydrophobic interactions, and one hydrogen bond was observed. Ritonavir and QQJ contained in 6vhn.pdb as its ligand both have one hydrogen bond. While T854 of the former forms H-bond, the latter does with M793. Sixteen residues of the ritonavir – EGFR complex participate in hydrophobic interactions with ritonavir and thirteen residues of 6vhn.pdb do. Hydrophobic interactions with six residues including G719, M766, M793, R841, D855, and G857 in the ritonavir – EGFR complex were not observed in the QQJ - 6vhn.pdb complex. Likewise, those with three residues including E791, L792, and P794 in 6vhn.pdb were not in the ritonavir – EGFR complex. The binding energy of ritonavir to the target protein EGFR is worse than that of QQJ to EGFR, however, because more residues participate in hydrophobic interactions, its docking results can compete with QQJ contained in 6vhn.pdb.

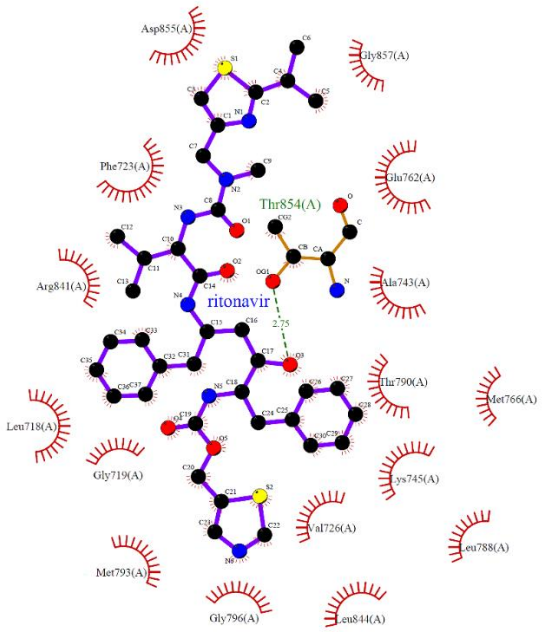

Fig. 18. Interactions between ritonavir and residues of 6vhn.pdb analyzed using the LigPlot program.

The off-targets effects of ritonavir were evaluated with the help of SwissTargetPrediction as listed in Table 3. More than a hundred proteins were provided as possible targets. Of them, eight proteins including Multidrug and toxin extrusion protein 1, Multidrug and toxin extrusion protein 2, Thromboxane-A synthase, Vasopressin V1a receptor, Neurokinin 2 receptor, Kappa Opioid receptor, Cytochrome P450 2C9, and Cytochrome P450 3A4 showed the probability of one and the others, less than 0.02. Among the proteins with non-zero probability, there is no EGFR.

Table 3. The target proteins of ritonavir predicted by SwissTargetPrediction web server.

Target	Target Class	Probability
Multidrug and toxin extrusion protein 1	Electrochemical transporter	1
Multidrug and toxin extrusion protein 2	Electrochemical transporter	1
Thromboxane-A synthase	Cytochrome P450	1
Vasopressin V1a receptor	Family A G protein-coupled receptor	1
Neurokinin 2 receptor	Family A G protein-coupled receptor	1
Kappa Opioid receptor	Family A G protein-coupled receptor	1
Cytochrome P450 2C9	Cytochrome P450	1
Cytochrome P450 3A4	Cytochrome P450	1
Acyl coenzyme A:cholesterol acyltransferase 1	Enzyme	0.02

Although ritonavir has concerns about off-target effects, it can be used with a repositioning drug for EGFR.

3.5. velpatasvir

The fifth drug ranked by the scoring function of LEA3D web server is velpatasvir, a HCV NS5A inhibitor, developed by Gilead. Its name is methyl N-[(1R)-2-[(2S,4S)-2-[5-[6-[(2S,5S)-1-[(2S)-2-(methoxycarbonylamino)-3-methylbutanoyl]-5-methylpyrrolidin-2-yl]-21-oxa-5,7-diazapentacyclo[11.8.0.03,11.04,8.014,19]henicosa-1(13),2,4(8),5,9,11,14(19),15,17-nonaen-17-yl]-1H-imidazol-2-yl]-4-(methoxymethyl)pyrrolidin-1-yl]-2-oxo-1-phenylethyl]carbamate, and its structure is shown in Fig. 19.

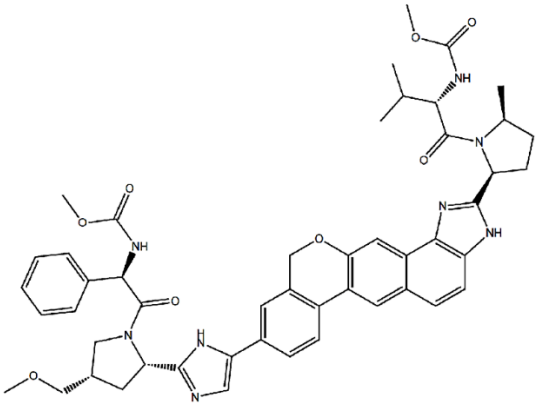

Fig. 19. The structure of velpatasvir, methyl N-[(1R)-2-[(2S,4S)-2-[5-[6-[(2S,5S)-1-[(2S)-2-(methoxycarbonylamino)-3-methylbutanoyl]-5-methylpyrrolidin-2-yl]-21-oxa-5,7-diazapentacyclo[11.8.0.03,11.04,8.014,19]henicosa-1(13),2,4(8),5,9,11,14(19),15,17-nonaen-17-yl]-1H-imidazol-2-yl]-4-(methoxymethyl)pyrrolidin-1-yl]-2-oxo-1-phenylethyl]carbamate.

The results obtained from *in silico* docking gave information about the bad binding energy (-5.3 kcal/mol ~ -3.1 kcal/mol) and bad docking poses. As shown in Fig. 20, velpatasvir is slightly draped over the opening of the binding site.

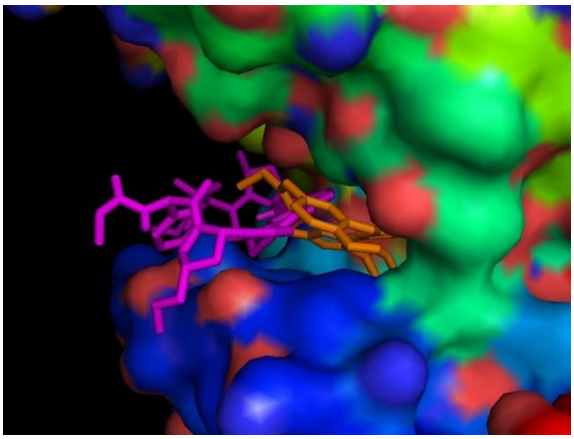

Fig. 20. Superimposition of velpatasvir (magenta) and QQJ (orange) contained in the binding pocket of 6vhn.pdb (EGFR) generated using the PyMol program.

Therefore, further experiments to confirm whether velpatasvir can be a drug to reposition for EGFR were not performed.

3.6. ombitasvir

Likewise, because the sixth drug ranked by the scoring function of LEA3D web server, ombitasvir showed bad docking results (the binding energy, -2.0 kcal/mol), further experiments were not carried out.

3.7. cobicistat

The scoring function of LEA3D web server provided cobicistat as the seventh candidate for repositioning. It inhibits human cytochrome P450 3A protein [24]. Its brand name is Tybost and its International Union of Pure and Applied Chemistry (IUPAC) name is 1,3-thiazol-5-ylmethyl N-[(2R,5R)-5-[[(2S)-2-[[methyl-[(2-propan-2-yl-1,3-thiazol-4-yl)methyl]carbamoyl]amino]-4-morpholin-4-ylbutanoyl]amino]-1,6-diphenylhexan-2-yl]carbamate whose structure is shown in Fig. 21. It was approved for the treatment of HIV-1 infection with other antiretroviral agents by FDA in 2012 (FDA Reference ID: 4145239, 2012).

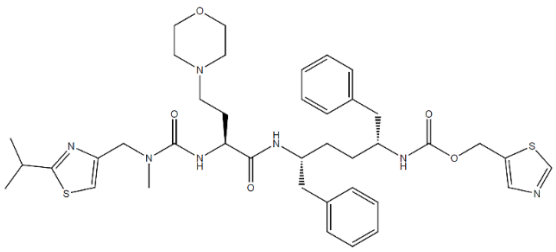

Fig. 21. The structure of cobicistat, 1,3-thiazol-5-ylmethyl N-[(2R,5R)-5-[[(2S)-2-[[methyl-[(2-propan-2-yl-1,3-thiazol-4-yl)methyl]carbamoyl]amino]-4-morpholin-4-ylbutanoyl]amino]-1,6-diphenylhexan-2-yl]carbamate.

Like other drugs mentioned above, *in silico* docking was performed. The binding energy ranged between -7.3 kcal/mol and -6.4 kcal/mol, and as shown in Fig. 22, its docking pose was superimposed with QQJ contained in 6vhn.pdb (EGFR) as its ligand well. The RMSD between 6vhn.pdb and the EGFR holo-protein – cobicistat complex was 2.7Å.

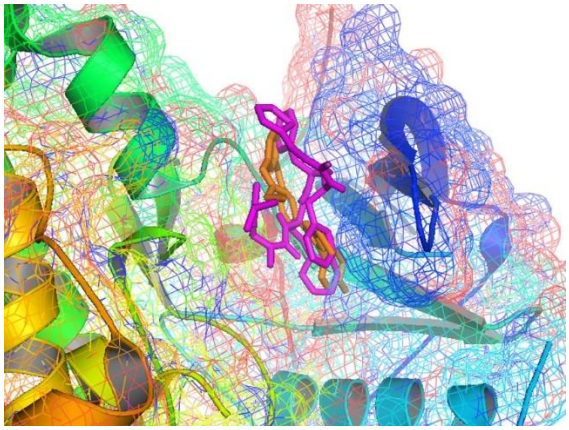

Fig. 22. Superimposition of cobicistat (magenta) and QQJ (orange) contained in the binding pocket of 6vhn.pdb (EGFR) generated using the PyMol program.

The LigPlot analysis revealed that fifteen hydrophobic interactions between cobicistat and the residues of EGFR were involved as follows: L718, G719, F723, V726, A743, K745, E762, M766, T790, M793, C797, D800, R841, L844, and D855 [Fig. 23]. However, hydrogen bond was not observed. Even though two more residues participate in hydrophobic interactions than QQJ contained in 6vhn.pdb, because of no hydrogen bond and its slightly worse binding energy, the docking condition of cobicistat cannot be considered to compete with QQJ.

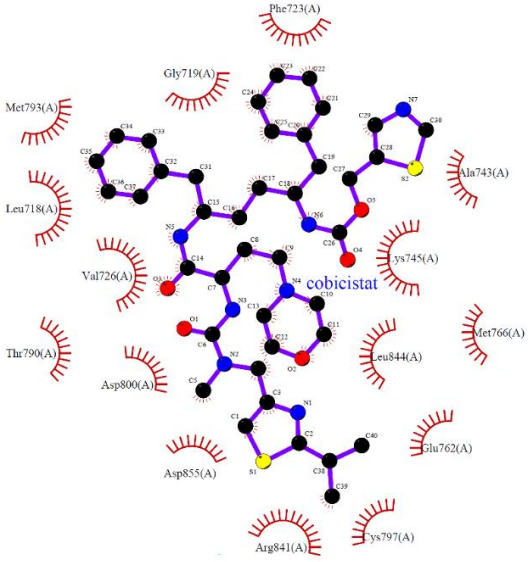

Fig. 23. Hydrophobic interactions between cobicistat and residues of 6vhn.pdb analyzed using the LigPlot program.

The off-target effects of cobicistat were predicted using SwissTargetPrediction web server. Fourteen proteins were suggested to be a target of cobicistat [Table 4]. The probability of all target proteins was less than 0.07, so that it can be considered that cobicistat does not show any off-target effect.

Table 4. The target proteins of cobicistat predicted by SwissTargetPrediction web server.

Target	Target Class	Probability
Multidrug and toxin extrusion protein 1	Electrochemical transporter	0.07
Multidrug and toxin extrusion protein 2	Electrochemical transporter	0.07
Thromboxane-A synthase	Cytochrome P450	0.07
Kappa Opioid receptor	Family A G protein-coupled receptor	0.07
Cytochrome P450 2C9	Cytochrome P450	0.07
Cytochrome P450 3A4	Cytochrome P450	0.07
Neurokinin 2 receptor	Family A G protein-coupled receptor	0.06
Vasopressin V1a receptor	Family A G protein-coupled receptor	0.05
Estradiol 17-beta-dehydrogenase 3	Enzyme	0.04
Cathepsin S	Protease	0.04
Platelet activating factor receptor	Family A G protein-coupled receptor	0.04
FK506-binding protein 1A	Isomerase	0.04
FK506 binding protein 4	Enzyme	0.04
p53-binding protein Mdm-2	Other nuclear protein	0.04

Therefore, cobicistat can be a repositioning drug for EGFR based on the results obtained from *in silico* docking, the interactions between the ligand and the protein, and target prediction.

3.8. aripiprazole lauroxil

Aripiprazole lauroxil developed by Alkermes is the eighth drug suggested by LEA3D web server. It is a prodrug of aripiprazole and its brand name is Aristada. Aripiprazole lauroxil was approved for the treatment of schizophrenia by FDA in 2015 (FDA Reference ID: 3829516, 2015) [25]. Its IUPAC name is [7-[4-[4-(2,3-dichlorophenyl)piperazin-1-yl]butoxy]-2-oxo-3,4-dihydroquinolin-1-yl]methyl dodecanoate and its structure is shown in Fig. 24.

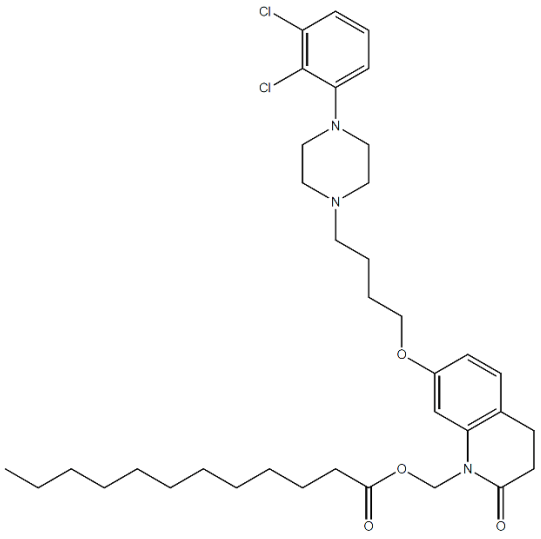

Fig. 24. The structure of aripiprazole lauroxil, [7-[4-[4-(2,3-dichlorophenyl)piperazin-1-yl]butoxy]-2-oxo-3,4-dihydroquinolin-1-yl]methyl dodecanoate.

In order to confirm whether aripiprazole lauroxil is docked into EGFR, *in silico* docking was carried out. Its binding energy ranged between -6.4 kcal/mol and -5.7 kcal/mol. The RMSD between 6vhn.pdb and the

EGFR holo-protein – aripiprazole lauroxil complex was 3.6Å. As shown in Fig. 25, it was docked into EGFR well.

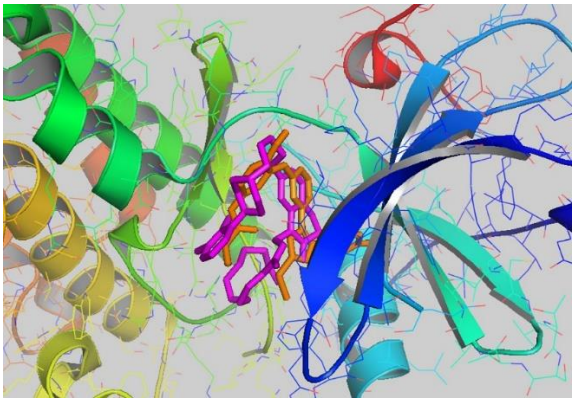

Fig. 25. Superimposition of aripiprazole lauroxil (magenta) and QQJ (orange) contained in the binding pocket of 6vhn.pdb (EGFR) generated using the PyMol program.

The interactions between aripiprazole lauroxil and EGFR were analyzed using LigPlot. Fifteen hydrophobic interactions were observed as follows: L718, F723, V726, A743, K745, T790, L792, M793, P794, G796, C797, N842, L844, T854, and D855 [Fig. 26]. Among residues participating in hydrophobic interactions between aripiprazole lauroxil and 6vhn.pdn (EGFR), five residues including M793, C797, N842, T854, and D855 are found in the residues participating in hydrophobic interactions between QQJ and EGFR. On the other way, three residues including E762, L788, and E791 participating in hydrophobic interactions of the QQJ – EGFR complex are not observed in residues participating in hydrophobic interactions of the aripiprazole lauroxil - EGFR complex. Even in the case of aripiprazole lauroxil, the number of residues participating in hydrophobic interactions is more than that in QQJ, because the binding energy of aripiprazole lauroxil to EGFR is worse than that of QQJ, the docking condition of aripiprazole lauroxil cannot be considered to be better than that of QQJ.

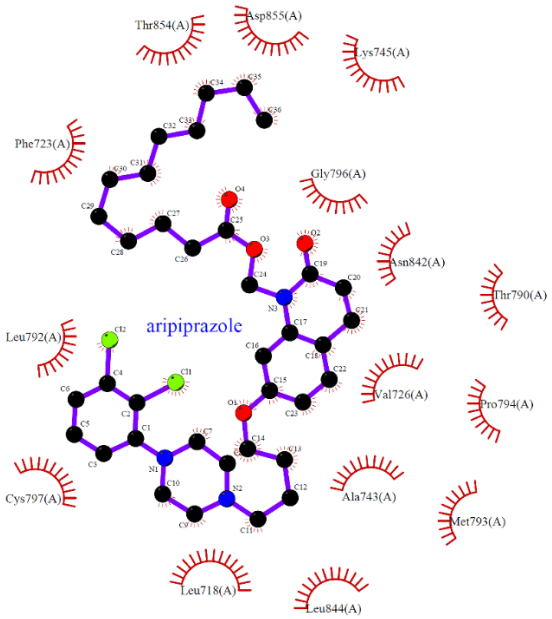

Fig. 26. Hydrophobic interactions between aripiprazole lauroxil and residues of 6vhn.pdb analyzed using the LigPlot program.

The off-target effects of aripiprazole lauroxil was analyzed with the help of SwissTargetPrediction web server. Forty-three proteins have been suggested to be targets for aripiprazole lauroxil. However, as listed in

Table 5, the protein with the greatest probability has a value of 0.07. Therefore, it can be considered that the off-target effects of aripiprazole lauroxil may be ignored.

Table 5. The target proteins of aripiprazole lauroxil predicted by SwissTargetPrediction web server.

Target	Target Class	Probability
P-glycoprotein 1	Primary active transporter	0.07
Serotonin 2c (5-HT2c) receptor	Family A G protein-coupled receptor	0.06
Dopamine D2 receptor	Family A G protein-coupled receptor	0.06

As a result, aripiprazole lauroxil can be a candidate for the repositioning of EGFR based on the results of *in silico* docking, the analysis of interactions between the compound and EGFR, and the off-target effects.

3.9. salmeterol

Salmeterol was the ninth drug suggested by LEA3D web server. It was approved as salmeterol xinafoate by FDA in 1994 (FDA Reference ID: 4465795, 1994). Its brand name is Serevent diskus which consists of salmeterol, 2-(hydroxymethyl)-4-[1-hydroxy-2-[6-(4-phenylbutoxy)hexylamino]ethyl]phenol [Fig. 27], and xinafoate, 1-hydroxynaphthalene-2-carboxylic acid. Because LEA3D web server suggested salmeterol, the current study for drug repositioning was carried out with a focus on salmeterol. A long-acting β2 adrenergic receptor agonist, salmeterol was approved for the treatment of asthma, and was developed by GlaxoSmithKline [26].

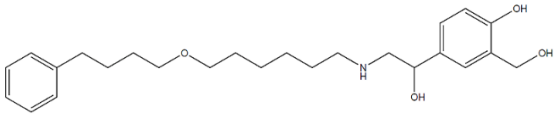

Fig. 27. The structure of salmeterol, 2-(hydroxymethyl)-4-[1-hydroxy-2-[6-(4-phenylbutoxy)hexylamino]ethyl]phenol.

In order to confirm whether salmeterol binds to EGFR, *in silico* docking was performed. It resulted in the binding energy ranging from -6.2 kcal/mol to -5.7 kcal/mol. The RMSD between 6vhn.pdb and the EGFR holo-protein – salmeterol complex was 1.4Å. As show in Fig. 28, it was docked into the binding pocket of EGFR and superimposed with QQJ contained in 6vhn.pdb as its ligand well.

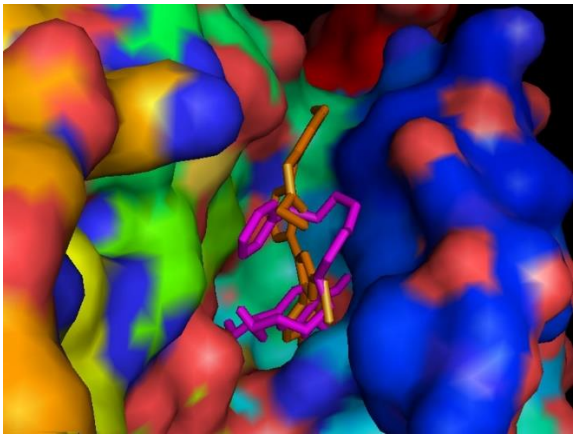

Fig. 28. Superimposition of salmeterol (magenta) and QQJ (orange) contained in the binding pocket of 6vhn.pdb (EGFR) generated using the PyMol program.

Because salmeterol showed good docking results including the binding energy as well as docking pose, the interactions with the residues of EGFR were analyzed using the LigPlot program. Thirteen residues including L718, F723, V726, A743, I744, K745, E762, L788, I789, T790, C797, R841, and L844 were observed in the hydrophobic interactions between salmeterol and EGFR [Fig. 29]. In addition to hydrophobic interactions, two hydrogen bonds were formed: between δ-hydroxy group of D855 and nitrogen of hexylamino group of salmeterol (2.94Å), and between hydroxy group of T845 and hydroxy group of hydroxyethyl group of salmeterol (2.84Å). The number of residues participating in hydrophobic interactions in the salmeterol – EGFR

complex is the same as that in the QQJ – EGFR complex (6vhn.pdb). Since one more hydrogen bond is formed in salmeterol than in QQJ, stronger docking conditions can be expected. However, the lower binding energy value offsets this advantage.

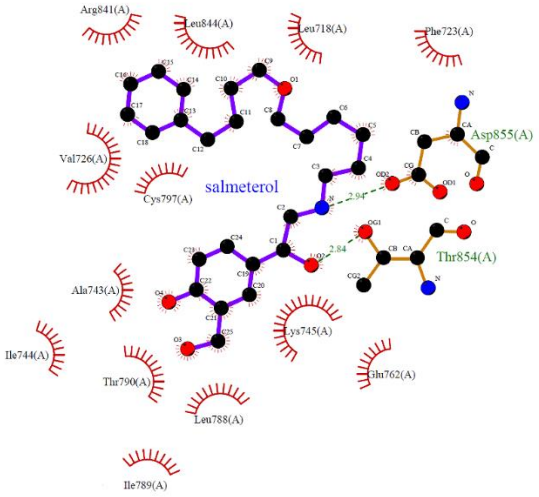

Fig. 29. Interactions between salmeterol and residues of 6vhn.pdb analyzed using the LigPlot program. Here the crescent-shaped red mark denotes the residues participating in hydrophobic interactions, and the green dotted lines represent hydrogen bonds.

Nineteen proteins were predicted to be targets of salmeterol by SwissTargetPrediction web server. Of them, four proteins showed probability of 1 as listed in Table 6. However, three proteins including Adrenergic receptor beta, Beta-1 adrenergic receptor, and Beta-3 adrenergic receptor belong to adrenergic receptors. This is a natural result since salmeterol is already known to be β2 adrenergic receptor antagonist. Others have less probability value than 0.11.

Table 6. The target proteins of salmeterol predicted by SwissTargetPrediction web server.

Target	Target Class	Probability
Adrenergic receptor beta	Family A G protein-coupled receptor	1
Beta-1 adrenergic receptor	Family A G protein-coupled receptor	1
Dopamine D3 receptor	Family A G protein-coupled receptor	1
Beta-3 adrenergic receptor	Family A G protein-coupled receptor	1
Glutamate [NMDA] receptor subunit epsilon 2	Ligand-gated ion channel	0.11

As a result, salmeterol can be a candidate for repositioning drug of EGFR.

Even though LEA3D web server has determined the rankings for 2058 drugs approved by the FDA, research only on drugs up to nineth place was conducted because the current study was performed using only *in silico* experiments. *In vitro* or *in vivo* experiments may be carried out for further study to confirm the current results in the near future. Unlike *in silico* experiments, *in vitro* or in vivo experiments have various limitations, so it is difficult to perform *in vitro* or *in vivo* experiments on many drugs.

In conclusion, fulvestrant, saquinavir, ritonavir, cobicistat, aripiprazole lauroxil, and salmeterol can be suggested to be repositioning drugs of EGFR. *In vitro* or *in vivo* experiments to confirm whether these dugs inhibit EGFR are remained for further study.

Acknowledgment: The paper was supported by Eswatini Medical Christian University.

Conflicts of Interest: The author has no conflict of interest related to this study to disclosure.

References

1. Siegel RL, Miller KD, Jemal A. Cancer statistics, 2016. CA Cancer J Clin. 2016;66(1):7-30.
2. Goel S, Hidalgo M, Perez-Soler R. EGFR inhibitor-mediated apoptosis in solid tumors. J Exp Ther Oncol. 2007;6(4):305-20.
3. Scagliotti GV, Selvaggi G, Novello S, Hirsch FR. The biology of epidermal growth factor receptor in lung cancer. Clin Cancer Res. 2004;10(12 Pt 2):4227s-4232s.
4. Agustoni F, Suda K, Yu H, Ren S, Rivard CJ, Ellison K, Caldwell C Jr, Rozeboom L, Brovsky K, Hirsch FR. EGFR-directed monoclonal antibodies in combination with chemotherapy for treatment of non-small-cell lung cancer: an updated review of clinical trials and new perspectives in biomarkers analysis. Cancer Treat Rev. 2019;72:15-27.
5. Burgess AW, Cho HS, Eigenbrot C, Ferguson KM, Garrett TP, Leahy DJ, Lemmon MA, Sliwkowski MX, Ward CW, Yokoyama S. An open-and-shut case? Recent insights into the activation of EGF/ErbB receptors. Mol Cell. 2003;12(3):541-52.
6. Hynes NE, MacDonald G. ErbB receptors and signaling pathways in cancer. Curr Opin Cell Biol. 2009;21(2):177-84.
7. Mendelsohn J. Targeting the epidermal growth factor receptor for cancer therapy. J Clin Oncol. 2002;20(18 Suppl):1S-13S.
8. Abourehab MAS, Alqahtani AM, Youssif BGM, Gouda AM. Globally Approved EGFR Inhibitors: Insights into Their Syntheses, Target Kinases, Biological Activities, Receptor Interactions, and Metabolism. Molecules. 2021;26(21):6677.
9. https://www.fda.gov/patients/learn-about-drug-and-device-approvals/drug-development-process
10. Sun D, Gao W, Hu H, Zhou S. Why 90% of clinical drug development fails and how to improve it? Acta Pharm Sin B. 2022;12(7):3049-3062.
11. Xue H, Li J, Xie H, Wang Y. Review of Drug Repositioning Approaches and Resources. Int J Biol Sci. 2018;14(10):1232-1244.
12. Benson G. Nucleic Acids Research annual Web Server Issue in 2010. Nucleic Acids Res. 2010;38(Web Server issue):W1-2.
13. Heppner DE, Günther M, Wittlinger F, Laufer SA, Eck MJ. Structural Basis for EGFR Mutant Inhibition by Trisubstituted Imidazole Inhibitors. J Med Chem. 2020;63(8):4293-4305.
14. Trott O, Olson AJ. AutoDock Vina: improving the speed and accuracy of docking with a new scoring function, efficient optimization, and multithreading. J Comput Chem. 2010;31(2):455-61.
15. Pettersen EF, Goddard TD, Huang CC, Couch GS, Greenblatt DM, Meng EC, Ferrin TE. UCSF Chimera--a visualization system for exploratory research and analysis. J Comput Chem. 2004;25(13):1605-12.
16. Kim JH, Ahn S, Koh D, Lee YH, Lim Y, Shin SY. 3-(5-hydroxyphenyl)-5-phenyl-2-pyrazolines as Toll-like receptor 7 agonists. J Chem. 2023;2151669.
17. Wallace AC, Laskowski RA, Thornton JM. LIGPLOT: A program to generate schematic diagrams of protein-ligand interactions. Prot Eng. 1995;8:127-134.
18. Daina A, Michielin O, Zoete V. SwissTargetPrediction: updated data and new features for efficient prediction of protein targets of small molecules. Nucleic Acids Res. 2019;47(W1):W357-W364.
19. Narayan P, Prowell TM, Gao JJ, Fernandes LL, Li E, Jiang X, Qiu J, Fan J, Song P, Yu J, Zhang X, King-Kallimanis BL, Chen W, Ricks TK, Gong Y, Wang X, Windsor K, Rhieu SY, Geiser G, Banerjee A, Chen X, Reyes Turcu F, Chatterjee DK, Pathak A, Seidman J, Ghosh S, Philip R, Goldberg KB, Kluetz PG, Tang S, Amiri-Kordestani L, Theoret MR, Pazdur R, Beaver JA. FDA Approval Summary: Alpelisib Plus Fulvestrant for Patients with HR-positive, HER2-negative, PIK3CA-mutated, Advanced or Metastatic Breast Cancer. Clin Cancer Res. 2021;27(7):1842-1849.
20. Ferencz E, Kovács B, Boda F, Foroughbakhshfasaei M, Kelemen ÉK, Tóth G, Szabó ZI. Simultaneous determination of chiral and achiral impurities of ivabradine on a cellulose tris(3-chloro-4-methylphenylcarbamate) chiral column using polar organic mode. J Pharm Biomed Anal. 2020;177:112851.
21. Balasubramaniam M, Reis RJS. Computational target-based drug repurposing of elbasvir, an antiviral drug predicted to bind multiple SARS-CoV-2 proteins. ChemRxiv. 2020;doi: 10.26434/chemrxiv.12084822.
22. Pereira M, Vale N. Saquinavir: From HIV to COVID-19 and Cancer Treatment. Biomolecules. 2022;12(7):944.
23. Lamb YN. Nirmatrelvir Plus Ritonavir: First Approval. Drugs. 2022;82(5):585-591.

24. von Hentig N. Clinical use of cobicistat as a pharmacoenhancer of human immunodeficiency virus therapy. HIV AIDS (Auckl). 2015;8:1-16.
25. Maini K, Gould H, Hicks J, Iqbal F, Patterson J 2nd, Edinoff AN, Cornett EM, Kaye AM, Viswanath O, Urits I, Kaye AD. Aripiprazole Lauroxil, a Novel Injectable Long-Acting Antipsychotic Treatment for Adults with Schizophrenia: A Comprehensive Review. Neurol Int. 2021;13(3):279-296.
26. Moore RH, Millman EE, Godines V, Hanania NA, Tran TM, Peng H, Dickey BF, Knoll BJ, Clark RB. Salmeterol stimulation dissociates beta2-adrenergic receptor phosphorylation and internalization. Am J Respir Cell Mol Biol. 2007;36(2):254-61.